Cement and Concrete Research 41 (2011) 964–974

Contents lists available at ScienceDirect

Cement and Concrete Research

journal homepage: http://ees.elsevier.com/CEMCON/default.asp

Derivation of a crack opening deflection relationship for fibre reinforced concrete panels using a stochastic model: Application for predicting the flexural behaviour of round panels using stress crack opening diagrams

Ali Nour [a,b,*], Bruno Massicotte [a], Renaud De Montaignac [a], Jean-Philippe Charron [a]

[a] Civil, Geological, and Mining Engineering Department, Ecole Polytechnique of Montréal, P.O. Box 6079, Station Centre-ville, Montreal, Québec, Canada H3C 3A7
[b] Hydro Québec, Montréal, Québec, Canada, H2L 4P5

ARTICLE INFO

Article history:
Received 27 October 2010
Accepted 9 May 2011

Keywords:
Bending strength (C)
Tensile properties (C)
Fiber reinforcement (E)
Modeling (E)
Monte Carlo simulation

ABSTRACT

This study is aimed at proposing a simple analytical model to investigate the post-cracking behaviour of FRC panels, using an arbitrary tension softening, stress crack opening diagram, as the input. A new relationship that links the crack opening to the panel deflection is proposed. Due to the stochastic nature of material properties, the random fibre distribution, and other uncertainties that are involved in concrete mix, this relationship is developed from the analysis of beams having the same thickness using the Monte Carlo simulation (MCS) technique. The softening diagrams obtained from direct tensile tests are used as the input for the calculation, in a deterministic way, of the mean load displacement response of round panels. A good agreement is found between the model predictions and the experimental results.

1. Introduction

The use of fibre reinforced concrete (FRC) as a construction material has continuously grown over the last decades due to its economical advantages in labour and material costs compared to conventional reinforced concrete. Randomly distributed fibres in concrete also contribute to the enhancement of the concrete post-cracking properties and durability when well proportioned and good quality FRC mixes are used. Fibres significantly prevent shrinkage cracking, reduce brittleness due to impact loading, compression or in unreinforced members subjected to shear or tensile forces, control cracking propagation, improve water tightness, etc. For these reasons, FRC has been successfully used in shotcrete, precast concrete, elevated slabs, bridge decks, pavements, industrial floors, seismic resisting structures, repair, etc.

The post-crack behaviour of FRC has been experimentally investigated based on a variety of tests. Although the actual post-cracking response of FRC is better defined by the stress–crack width $\sigma(W)$ relationship measured in a direct tension test, the vast majority of reported test results in the literature involve beams due to the ease of performing bending tests. Flexural beam tests [2], however, have two main disadvantages: the $\sigma(W)$ relationship cannot be obtained directly and tests on small FRC elements engender important scatters in the results that are not representative of the actual in situ conditions [7]. Those observations encouraged many investigators to perform tests on FRC square or round panels of large dimension [1,12,13,17,20]. Despite the better representation of concrete volumes in panel tests, the actual post-cracking behaviour of FRC in tension cannot be determined satisfactory using analytical approaches by any of the proposed tests in the literature unless the softening mechanism is well understood, and the level of deformation and strain-softening characteristics of the material are known.

Contributions in the literature dealing with the post-crack response determination of FRC panels using simple approaches are very limited. Marti et al. [20] developed a simple theoretical approach that accounts for the random fibre distribution for the analysis of slabs. Their model is based a priori on a predefined parabolic softening relationship that considerably simplifies the derivation of load–deflection curves from yield line theory. Recently, Khaloo and Afsari [17] used the same approach for analyzing their tested slabs. Tran et al. [30] proposed an interesting formulation for determining the nonlinear load–deflection response of the round panel [1]. Their formulation uses the yield line theory based on the flexural capacity of beams of similar composition and thickness. They did not use an explicit stress crack–opening relationship; they rather adopted the moment crack rotation angle response of beams as the input.

For the case of FRC beams, Zhang and Stang [32] proposed an analytical formulation that provides, with satisfactory accuracy, the load–displacement response for an arbitrary inputted stress crack-opening diagram. They use an additional relationship derived from fracture mechanics that links the crack mouth opening displacement (CMOD) to the external moment and the crack parameter. For the case

* Corresponding author at: Civil, Geological and Mining Engineering Department, Ecole Polytechnique of Montréal, B.O. Box 6079, Station Centre-ville, Montreal, Québec, Canada H3C 3A7. Tel.: +1 514 340 4711x4109; fax: +1 514 340 5881.
E-mail address: ali.nour@polymtl.ca (A. Nour).

0008-8846/$ – see front matter © 2011 Elsevier Ltd. All rights reserved.
doi:10.1016/j.cemconres.2011.05.003

of FRC panels, to the authors' knowledge, similar analytical formulation is either scarce or does not exist, whereas such an additional relationship is very difficult to derive analytically.

This study is, therefore, aimed at proposing a simple analytical formulation to investigate the post-crack behaviour of the FRC panels of rectangular or circular geometry using an arbitrary tension softening stress crack opening diagram as the input. The formulation assumes a symmetrical or axisymmetrical crack pattern. The present paper proposes a new relation to link the crack opening to the panel deflection that is required for predicting the round panel response. Due to the stochastic nature of material properties, the random fibre distribution, and other uncertainties that are involved in concrete mix, deterministic approaches are not suitable for deriving that additional relationship for panels. The resorting to probabilistic techniques enables modeling uncertainties and analyzing their dispersion effects. In this context, the load deflection response is predicted using the yield line theory based on the crack length parameter-normalized deflection diagram that was developed from the analysis of beams having the same thickness using the Monte Carlo simulation (MCS) technique.

The proposed approach is applied to round determinate panels, and the results obtained are compared to the experimental results. Mean softening diagrams obtained from the direct tension test are used as the input to calculate, in a deterministic way, of the mean load displacement response.

2. Model derivation for the flexural analysis of FRC panels

There is limited published information on analytical techniques that are suitable for predicting the complete flexural history of panels made of strain-softening FRC. Classical yield line theory [15,29] can only predict the maximum load because it assumes that the level of resistance offered by the chosen collapse mechanism remains constant over the range of deformations. If the resistance of a component within an assumed mechanism changes as the load is introduced, the work carried out in resisting the external load is altered and the overall capacity will change. The magnitude of the change in the load capacity can be determined if the level of deformation and strain-softening characteristics of the material are known.

The model adopted in the present study is based on the yield line approach. In the initial stage, the behaviour is assumed to be elastic until the maximum tensile stress reaches concrete cracking strength. Beyond that point, the model assumes that several fictitious cracks may develop depending on the failure pattern of the analyzed panel. Fig. 1 shows a typical stress distribution at the cracked panel section.

The fictitious crack develops when the tensile stress reaches its ultimate value and spreads along a part of the panel thickness h. After the crack has initiated, the fictitious crack progresses and the material is softened by cohesive forces in the fracture process zone where a nonlinear $\sigma(W)$ relationship is used as shown in Fig. 1.

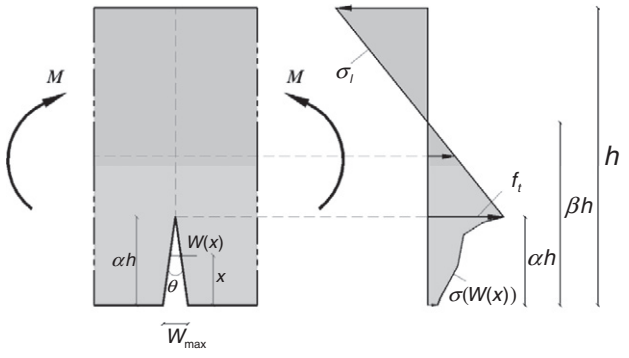

Fig. 1. Stress distribution at cracked panel section.

When the crack opening displacement (COD) W reaches a critical value W_C, the stress transfer becomes zero and a real crack starts to grow freely. Because the FRC structure behaviour is dominated by tensile cracking, one assumes that the compression behaviour is linearly elastic. The same cracked section proposed in Ref. [32] for beams is adopted in the present study where it is assumed that the crack has a linear profile:

$$W = W_{max}\cdot\left(1-\frac{x}{\alpha\cdot h}\right) \tag{1}$$

for which:

$$W_{max} = \frac{\sum_{i=1}^{n_c} W_{max,i}}{n_c} \tag{2}$$

W_{max} is the mean crack mouth opening displacement (CMOD), n_c is the number of cracks depending on the chosen failure pattern. Therefore, W is the mean crack opening displacement at location x, and αh is the mean crack length for which the parameter $\alpha\in[0, 1]$. With these assumptions, $\sigma(W)$ represents the mean softening diagram of the panel. From the equilibrium conditions, we have:

$$\int_0^{\alpha h}\sigma(W(x))\cdot dx + \int_{\alpha h}^{h}\sigma_l(x)\cdot dx = 0 \tag{3.a}$$

$$\int_0^{\alpha h}\sigma(W(x))\cdot(h-x)\cdot dx + \int_{\alpha h}^{h}\sigma_l(x)\cdot(h-x)\cdot dx = M \tag{3.b}$$

M is the panel resisting moment per unit of length along the yield line. It is assumed to be uniform along the crack and depends on the geometry and the chosen failure pattern of the analyzed panel. $\sigma(W(x))$ and $\sigma_l(x)$ are the normal stress functions in the cracked (nonlinear) and the uncracked (linear) parts, respectively. $\sigma(W(x))$ is related to αh, βh and W_{max} using the σ-W relationship together with Eq. (1), i.e.:

$$\sigma(W(x)) = \sigma\left(W_{max}\cdot\left(1-\frac{x}{\alpha\cdot h}\right)\right) \tag{4}$$

$\sigma_l(x)$ can be related with αh, βh and W_{max} as follow:

$$\sigma_l(x) = f_t\cdot\left(1-\frac{x-\alpha\cdot h}{\beta\cdot h-\alpha\cdot h}\right) \tag{5}$$

where βh is the depth of the tensile zone, $\beta\in[0.5, 1]$ and it is determined by introducing Eq. (5) into Eq. (3.a):

$$\beta = \frac{\alpha\cdot\int_0^{\alpha h}\sigma(W(x))\cdot dx + 0.5\cdot f_t\cdot h\cdot\left(1-\alpha^2\right)}{\int_0^{\alpha h}\sigma(W(x))\cdot dx + f_t\cdot h\cdot(1-\alpha)} \tag{6}$$

One notes that the integrals of Eqs. (3.b) and (6) are numerically determined using the Gauss–Legendre technique.

According to the principle of virtual work, one can derive a relationship between the applied load F and the generated bending moment M as follow [15]:

$$\sum F\cdot\Delta = \sum M\cdot\theta\cdot L \tag{7}$$

Here Δ stands for the deflection, L is a characteristic length of the panel, and θ is the corresponding crack angle of rotation (in

radian) between the adjoining uncracked parts of the panel (Fig. 1). By modeling the crack as a generalized plastic hinge, θ can be estimated by:

$$\theta = \frac{W_{\max}}{\alpha \cdot h} \tag{8}$$

This approach requires an additional relation linking the crack length parameter α to the deflection Δ to obtain the complete solution between the external load and the deflection. In the case of beams under three point bending, Zhang and Stang [32] used a relationship derived analytically from fracture mechanics in which W_{max} is linked to the external moment M and the crack length parameter α. The load–deflection curve is determined by increasing the crack length parameter α and solving nonlinear equations through a simple bisection iteration scheme. For the case of round panels, when an arbitrary σ–W softening law is used as the input, such an additional relationship is difficult to derive analytically and, according to the authors' knowledge, has never been proposed.

Marti et al. [20] developed a theoretical approach based on a priori well defined parabolic softening relationship that accounts for the random fibre distribution for the analysis of square and circular panels under point loading with continuous simple supports along the perimeter. Such an assumption simplifies the derivation of load–deflection curves from the yield line theory (Eq. (7)). Recently in Ref. [17], the same approach was used for the analysis of square slabs on four corners.

In Ref. [30], the authors performed a series of analysis using the yield line theory to derive the nonlinear load–deflection response of the round panels [1] based on the flexural capacity of the beams of similar composition and thickness. They did not explicitly use a σ–W softening relationship as an input in their approach. Instead they use the moment crack rotation angle diagrams (M–θ) of beams as input. According to Eq. (7), the post-cracking load–deflection curve can be determined by increasing the displacement at the centre of the panel and, using the moment of resistance offered by beams at each corresponding crack rotation angle, the load at equilibrium for these moments can be found.

As reported by Refs. [3,18,32], the flexural performance of FRC materials is directly related to the σ–W diagram. This diagram is needed for structural design applications since it represents the energy change in the fracture process zone at the material level. Thus, the σ–W diagram is considered the characteristic material property of FRC materials. Standardized testing methods have adopted various types of bending tests for determining the characteristic behaviour of FRC related to the load displacement curves of FRC. For instance, the panels under the point load have been proposed by EFNARC [13] and ASTM [1], whereas a notch beam test has been standardized in the European Standard [14]. On the other hand, the test method to determine the tension softening diagrams has not yet been standardized. In practice, the simplest test method is to perform a direct tension test, as suggested in Ref. [27]. Unfortunately, it is not easy to control the crack propagation in a stable manner and symmetrical way [5,28]. Furthermore, such tests are complicated to perform since it is difficult to prepare the specimen, and to impose unambiguous boundary conditions in the setup [16]. The alternative that is currently being studied exhaustively is the use of the experimentally obtained F–Δ response of some structural elements to determine the σ–W curve of the corresponding material through inverse analysis. Most investigators have focused on the behaviour of a notched beam under a three point bending load, whereas an inverse analysis with FRC panels is very scarce in the literature. It is noteworthy that most available methods are using data fitting techniques combined in some occasions with optimization algorithms, for which the shape of the σ–W diagram is either fixed a priori or free to vary. In all cases, an analytical formulation that uses the σ–W curve as the input and provides the analytical load–displacement response is needed to match with the experimental results. For the case of FRC beams, the analytical formulation proposed in Ref. [32] is simple, easy to implement, and provides, with satisfactory accuracy, the load–displacement response for an arbitrary inputted σ-W diagram. For FRC panels, to the authors' knowledge, such an analytic formulation is either scarce or does not exist.

This study proposes a simple analytical formulation to investigate the post-crack behaviour of FRC panels using an arbitrary σ–W diagram as the input. The proposed post-crack behaviour of FRC panels is studied using the yield line theory, where the load deflection response is predicted based on the crack length parameter-normalized deflection relationship. The relationship is developed from the analysis of beams with the same thickness using the Monte Carlo simulation (MCS) technique, as described in the next section.

3. Crack length parameter-normalized deflection curve for beams using the MCS technique

3.1. Procedure

For deriving the additional relation, form Eq. (7), between the crack length parameter α and the deflection Δ, Tran et al. [30] used M–θ diagrams obtained from beam test results as the input to the numerical analysis for analyzing panels. It is in this way that the M–θ diagrams of beams implicitly represent the degree of strain-softening characteristic of the material and are considered as the constitutive models for analyzing the structural behaviour of the panel. In their analysis, a Monte Carlo simulation has been incorporated in order to account for the stochastic nature of the material properties.

The objective of the present study is to use any arbitrary σ–W diagram as the input for the numerical analysis of round panels. Because these diagrams are very difficult to be derived directly from round panel tests, one proposes to determine the α–Δ diagrams from the analysis of beams in a first step. In addition, because the maximum deflections observed in the panels are more important than for beams, the crack length parameter α is obtained as a function of the normalized displacement $\overline{\Delta}$. Here, $\overline{\Delta} = \Delta / \Delta_{max}$ where $\Delta_{\max}$ is the maximum analytical beam deflection. In the beam analysis, the following σ–W relationship is chosen for its generality and versatility:

$$\sigma(W) = f_t \cdot \left(1 - \frac{W}{W_C}\right)^N \tag{9}$$

The softening index N ($0<N<\infty$) allows Eq. (9) to cover all the types of engineering materials. For instance, with $N=0$ and $\sigma(W)=f_t$, Eq. (9) describes the behaviour of all the elastic-perfectly plastic solids, whereas $N=\infty$ and $\sigma(W)=0$ are appropriate to represent brittle materials without the softening region. Expressions obtained for $0<N<1$ are typical of ductile metals and polymers in plane stress conditions characterized by strain hardening behaviour [26]. For materials such as steel fibre reinforced concretes (SFRC), the softening index range is $1<N<\infty$ [4]. It is difficult to determine the value of N analytically if the softening mechanism is not well understood.

The beams are analyzed using the analytic formulation proposed in Ref. [32]. A preliminary investigation shows that for a given softening law, the beam depth has a slight influence on the α–$\overline{\Delta}$ diagram, whereas the inputted softening law significantly influences the required α–$\overline{\Delta}$ diagrams, in turn indicating that the material characteristic is of prime importance. Deterministic approaches are not suitable for deriving the α–$\overline{\Delta}$ formula for panels because of the stochastic nature of the material properties, random fibre distribution, and other uncertainties that are involved in concrete mix. The resort to probabilistic techniques enables modeling uncertainties and analyzing their dispersion effect. For this reason, a stochastic model is used to account for the randomness of the three variables f_t, W_C and N defining the adopted σ–W law.

In the present study, the FORTRAN 95 language has been used to develop a computer program for the derivation of α–$\overline{\Delta}$ diagrams for panels. The developed procedure integrates the analytic formulation proposed in Ref. [32] for beams combined with the Monte Carlo simulation technique.

3.2. Stochastic model for σ–W diagrams

For engineering purposes, one assumes that the variability of a given material property is decomposed into a deterministic trend, and a random component describing the variability about that trend. Tensile stress f_t, critical crack opening displacement W_C and softening index N in Eq. (9) are modeled herein as random variables. For the random simulation of these properties, the chosen random variables are defined by their moments of order 1 and 2, which are respectively the mean and variance. Let T_p standing for one typical random variable, defined as a function of the deterministic function T_{0p} describing the trend, taken in practice as the mean of measured values, and also the function of zero mean, unit variance Gaussian random variable ΔT_p. One can write:

$$T_p = \Re\left[T_{0p} + \tau_p \Delta T_p\right] \tag{10}$$

$\Re$ is a transformation taking the Gaussian process ΔT_p into the distribution appropriate for T_p and τ_p is the standard deviation. Here, $p=1$ corresponds to the softening index, $p=2$ for tensile stress, and $p=3$ for critical crack opening displacement. The random variable ΔT_p can be simulated as follow:

$$\Delta T_p = \sqrt{\frac{2}{K_p}} \cdot \sum_{l=1}^{K_p} cos\left(\Omega_{l,p}\right) \tag{11}$$

$$mean\left(\Delta T_p\right) = 0\,; \quad p = 1,3 \tag{12}$$

Ω_l is a random phase angle distributed uniformly over the interval [0, 2π]. K is a large enough integer. A stochastic independence between ft and the other random variables W_C and N is assumed, which is preferable versus selecting any erroneous correlation. In practice, there is a direct correlation between N and W_C. Small values of N are typical of a high fibre dosage leading to large values of W_C, whereas large values of N represent materials with a smaller fibre dosage (more brittle materials) leading to small values of W_C. For this reason, a stochastic correlation is considered between N and W_C.

3.2.1. Softening index variability

The softening index N is bounded in practice between two extreme values, namely, $N \in [N_{min} N_{max}]$. The beta distribution is appropriate in the case of random variable whose values are bounded. In the present paper, the technique is used that was well described by Nour et al. [23], for which the softening index variability expression is given by:

$$N = N_{min} + (N_{max} - N_{min}) V_N \tag{13}$$

The result, $V_N \in [0\ 1]$, is the solution of the integral equation of the beta cumulative distribution function (cdf) with parameters q and r where it supplied the desired probability $P_{\overline{V}_N}$ i.e.:

$$\mathrm{B}(V_N \,|\, q,r) = \frac{B_{V_N}(q,r)}{B(q,r)} = P_{\overline{V}_N}\,; q,r > 0 \tag{14}$$

Here, the simulated random variable $\overline{V}_N$ is transformed into the beta random variable N by mapping on the probability distribution function diagram. Through the mapping operation, the same mean and variance are used for determining q, r and $\overline{V}_N$. $B_{V_N}(q, r)$ is the incomplete beta function, and V_N is obtained by assuming that beta cdf is equal to an appropriate probability function $P_{\overline{V}_N}$. In this study, because the softening index is a positive parameter, one prefers to map the beta cdf with the lognormal cdf one, hence:

$$P_{\overline{V}_N} = \Phi_0\left(\frac{\ln \overline{V}_N - \ln\left(N_{0,N}\, exp\left(-\frac{1}{2}\tau^2_{\ln N}\right)\right)}{\tau_{\ln N}}\right) \tag{15}$$

where Φ_0 stands for the standard normal cumulative distribution function, and $\overline{V}_N$ is one to one mapping of $\overline{V}_N \in [0 + \infty]$ into $P_{\overline{V}_N} \in [0\ 1]$. $\overline{V}_N$ expression is given by:

$$\overline{V}_N = exp\left[N_{0,\ln N} + \tau_{\ln N} \cdot \Delta T_N\right] \tag{16}$$

with:

$$\tau^2_{\ln N} = \ln\left(1 + \frac{\tau^2_N}{N^2_{0,N}}\right); N_{0,\ln N} = \ln\left(N_{0,N}\right) - \frac{1}{2}\tau^2_{\ln N} \tag{17}$$

where N_0 and τ^2_N stand for the softening index mean and variance, respectively.

With this formulation, there exists a critical standard deviation to not exceed as given in Ref. [23]:

$$\tau_N < \tau_{N,cr} = \sqrt{(N_0 - N_{min}) \cdot (N_{max} - N_0)} \tag{18}$$

3.2.2. Tensile stress and critical crack opening displacement variability

The tensile stress and the critical crack opening displacement are assumed to be lognormally distributed. This choice is motivated by the fact that these parameters are positive, and that lognormal distribution enables the analyzing of their large variability. The tensile stress and crack opening displacement expressions are given by:

$$f_t = exp\left[\mu_{\ln f_t} + \tau_{\ln f_t} \cdot \Delta T_{f_t}\right] \tag{19.a}$$

$$W_C = exp\left[\mu_{\ln W_C} + \tau_{\ln W_C} \cdot \left(\Delta T_N \cdot R_{W_C N} + \Delta T_{W_C} \cdot \sqrt{1 - R^2_{W_C N}}\right)\right] \tag{19.b}$$

with:

$$\tau^2_{\ln f_t} = \ln\left(1 + \frac{\tau^2_{f_t}}{\mu^2_{f_t}}\right); \mu_{\ln f_t} = \ln\left(\mu_{f_t}\right) - \frac{1}{2}\tau^2_{\ln f_t} \tag{20}$$

$$\tau^2_{\ln W_C} = \ln\left(1 + \frac{\tau^2_{W_C}}{\mu^2_{W_C}}\right); \mu_{\ln W_C} = \ln\left(\mu_{W_C}\right) - \frac{1}{2}\tau^2_{\ln W_C}$$

where μ_{f_t}, μ_{W_C}, $\tau_{f_t}{}^2$ and $\tau_{W_C}{}^2$ respectively stand for tensile stress and crack opening displacement mean and variance. $R_{W_C N}$ stands for an inter-parameter correlation obtained from the following equation:

$$R_{W_C N} = \frac{mean(W_C \cdot N) - mean(W_C) \cdot mean(N)}{\tau_{W_C} \cdot \tau_N}; -1 \le R_{W_C N} \le 1 \tag{21}$$

The strategy simulation in Eq. (19.b) consists in first simulating the random variable N, followed by a simulation of the random variable W_C in correlation with N.

3.2.3. Numerical analysis for beams

The above described procedure is used to derive the crack length parameter-normalized deflection α–$\overline{\Delta}$ for beams to be used for panel analysis. Monte Carlo simulations are used to generate samples having characteristics close to specimens produced in the laboratory. It is reported in the literature that the variability of f_t is roughly in the same order as for the compression strength [19,21,22] and is around

$CV_{f_t} \approx 0.15$ to 0.25. The value of $CV_{f_t} \approx 0.32$ is reported in Ref. [6]. As stated in Ref. [9] and elsewhere in Ref. [25], CV_{f_t} could be greater than 0.4 for poor concrete, for this reason CV_{f_t} is varied in this study up to 0.5. For the critical crack opening displacement W_C, Chengqing [10] has reported that the variation coefficient for W_C is in the order of 40%. On the other hand, as indicated in Ref. [6], the variation coefficient for W_C is around 40% for concrete. Because the complete area of the σ–W curve is controlled by W_C, a variability of up to 40% for W_C seems reasonable. There is practically no available information on the variability of the softening index N. When the variation coefficient is close to $CV_{N,\,cr}$ ($CV_{N,\,cr} = N_0/\tau_{N,\,cr}$), the simulation provides samples concentrated at extreme values, which is not realistic. This situation could be avoided by choosing the variation coefficient equal to $0.5 \cdot CV_{N,\,cr}$[23]. Hence, the following data are used:

- Mean tensile stress: $\mu_{f_t} = 3.5$ MPa;
- Mean crack opening displacement corresponding to zero tensile strength $\mu_{W_c} = 8$ mm;
- $N_{\min} = 1$ and $N_{\max} = 7$ with the mean value $N_0 \in [N_{\min} N_{\max}]$.

Fig. 2a to c shows the typical histograms of N for three situations for N_0. The softening index N has a direct correlation with the parameters influencing the shape of the post-cracking load deflection response such as the type and volume of fibres or the quality of the concrete mix. For this reason, three representative practical conditions were considered. The first one represents specimens dominated by FRC mixes having a high percentage of fibres (Fig. 2a) idealized by samples of Monte Carlo simulations having N_0 close to $N_{\min}$ i.e. $N_0 = (3N_{\min} + N_{\max})/4 = 2.5$. The second condition considers specimens covering all the possible percentage of fibres (Fig. 2b), represented by the samples of Monte Carlo simulations having N_0 equal to the central value i.e. $N_0 = (N_{\min} + N_{\max})/2 = 4$. As shown by Fig. 2c, the third situation is the opposite of the first one with the majority of specimens made with low percentage of fibres, idealized by samples of Monte Carlo simulations having N_0 close to $N_{\max}$ i.e. $N_0 = (N_{\min} + 3N_{\max})/4 = 5.5$.

Typical histograms for f_t and W_C are plotted in Fig. 3 for which W_C histogram, as explained before and well illustrated by Fig. 4, is produced considering a strong negative correlation between N and W_C i.e. $R_{W_C N} = -0.75$. As it appears clearly in Fig. 3a, the selection of the tensile stress variability $CV_{f_t} = 0.5$ allows to model high, average and low strength concrete in Monte Carlo simulations.

Using Eqs. (9), (13), and (19), 1000 independent realizations of σ–W diagrams were randomly generated and were directly considered in Monte Carlo simulations of beam analysis. This exercise provides the required mean α–$\overline{\Delta}$ diagram to be used for panels. Fig. 5 illustrates 25 typical realizations of σ–W diagrams for the case of $N_0 = 4$ for which a strong negative correlation between N and W_C was considered, i.e. $R_{W_C N} = -0.75$.

The observed scatter from one realization to another is important, because the three key parameters in relation with the assumed softening law (Eq. (9)) are supposed to be uncertain. Fig. 6 illustrates the variability effect of ft, W_C and N on the mean load displacement curve for beam having $h = 75$ mm. When $N_0 = 4$, ft and W_C are varied each one at a time (Fig. 6a and b). One observes that they globally exert a slight influence on the post-crack response of the beam (Fig. 6a and b). Furthermore, one sees that as CV_{f_t} or CV_{W_c} increases, the beam capacity decreases, accompanied by a slight increase of the softening level in comparison with the deterministic case ($CV_{f_t} = CV_{W_c} = 0$). On the other hand, Fig. 6c shows the variability effect of the softening index N for which the three representative situations in relation with the fibre dosage were investigated. It is well shown that as the mean value N_0 increases, the softening character significantly increases and the load capacity of the beam decreases.

The results also indicate that for $N_0 = 4$, the randomness in N does not affect the beam capacity, but leads to a slight decrease of the softening level in comparison with the deterministic case ($CV_N = 0$). The same remarks were obtained for $N_0 = 2.5$ and $N_0 = 5.5$.

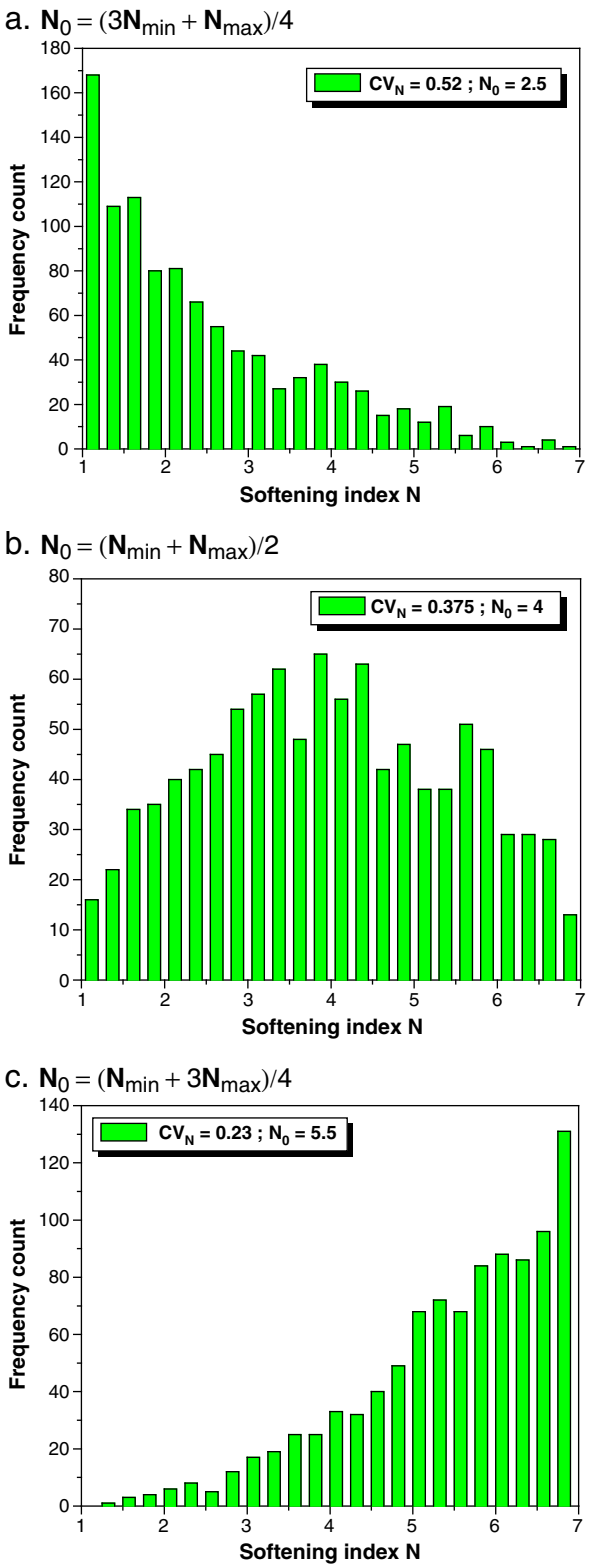

Fig. 2. Typical histograms for N.

In this study, for a given beam depth h, the required α–$\overline{\Delta}$ diagrams were determined with 1,000 Monte Carlo simulations for each representative situation of N_0 ($N_0 = 2.5$, 4 and 5.5). This allows for covering a maximum range of fibre dosage. In Fig. 7, 3000 samples of Monte Carlo simulations are superimposed altogether, each individual 1000 samples corresponding to the following data:

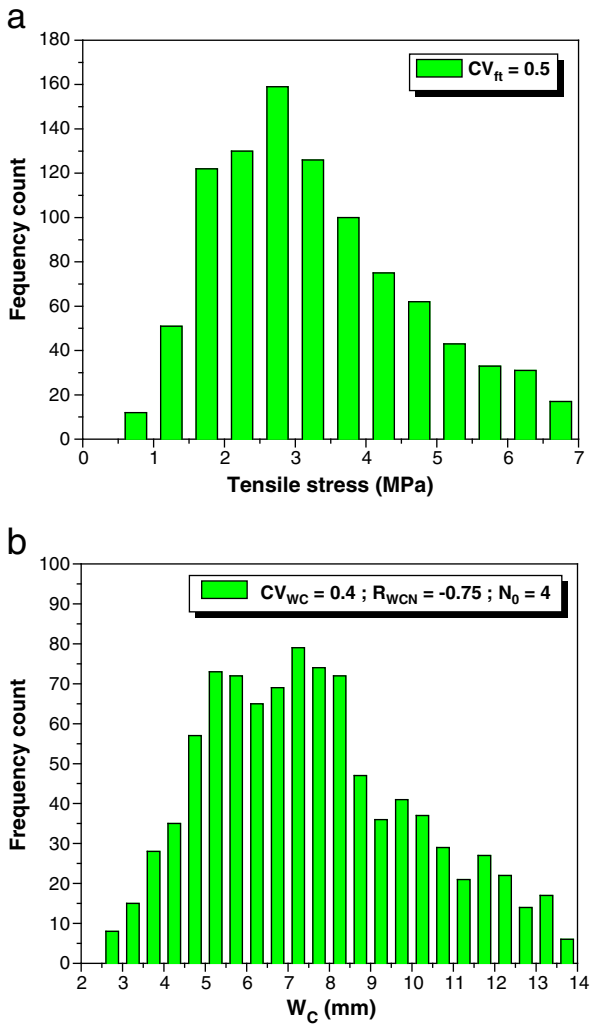

Fig. 3. Typical histograms for f_t and W_C.

- $CV_{ft} = 0.5Z$; $CV_{W_c} = 0.4$; $N_0 = 2.5$ and $CV_N = 0.52$.
- $CV_{ft} = 0.5Z$; $CV_{W_c} = 0.4$; $N_0 = 4$ and $CV_N = 0.375$.
- $CV_{ft} = 0.5Z$; $CV_{W_c} = 0.4$; $N_0 = 5.5$ and $CV_N = 0.23$.

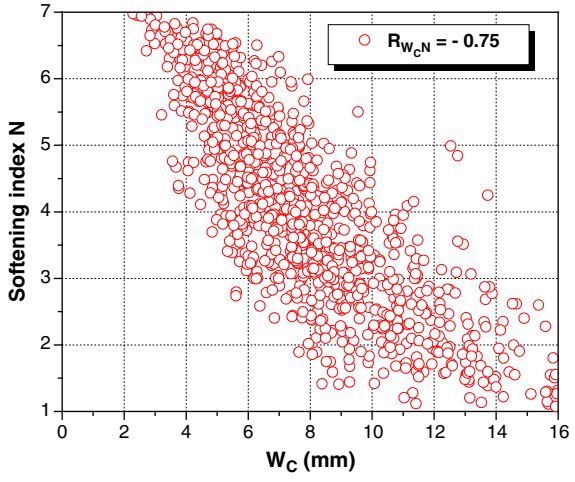

Fig. 4. Negative correlation between N and W_C ($N_0 = 4$, $CV_N = 0.375$ and $CV_{W_c} = 0.4$).

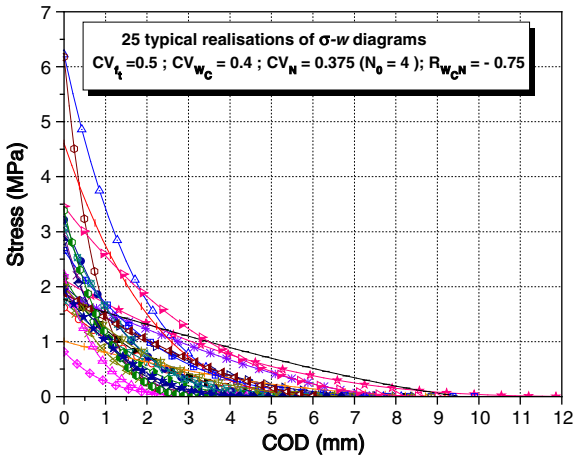

Fig. 5. Typical realizations of σ–W diagrams (COD: crack opening displacement).

As shown in Fig. 7, the randomness in ft, W_C and N produces a scatter in α–$\overline{\Delta}$ results with an interesting trend. This permits the easy fit of the results with an appropriate function. The function given by Eq. (22) was chosen because it accurately captures the full trend observed in the MCS results. The constants c_1, c_2, and c_3 are estimated using a nonlinear fitting scheme from the realizations ensemble, whereas the assumed function satisfactorily passed the Chi-square goodness of the fit test.

$$\alpha = \frac{c_1 \cdot \overline{\Delta}^{c_2}}{1 + c_3 \cdot \overline{\Delta}^{c_2}} \tag{22}$$

Results reported in Fig. 7 corresponds to $h = 75$ mm. The same routine was repeated for other beam depths, namely $h = 100$ mm and $h = 125$ mm. For the three selected beam depths, Fig. 8a, synthesizes the mean load displacement curve of 1000 samples corresponding to $N_0 = 4$, whereas Fig. 8b depicts the fitted α–$\overline{\Delta}$ diagrams based on 3000 realizations each. Their corresponding constants c_1, c_2 and c_3 are summarized in Table 1. Despite the beam thickness significantly influence the load capacity (Fig. 8a), it exerts relatively a slight influence of the α–$\overline{\Delta}$ diagram as shown by Fig. 8b. Values of c_1, c_2 and c_3 for depths between 75 and 125 mm could be easily obtained by interpolation from Table 1 data.

As a summary to this section, the stochastic model was used to develop Eq. (22) that links the crack length parameter to the panel deflection. In the next section, this equation is embedded into the mechanical model that was formulated using a mean cracked section based on a mean arbitrary σ–W softening law. Because exploring the dispersion is beyond the scope of this paper, only the mean load displacement response of the round panel is calculated in a deterministic way. In this case, the mean σ–W diagrams obtained from the direct tensile tests are used as the input.

4. Application to the round determinate panel and comparison with the experimental results

There is only very limited contributions available in the literature that deal with the F–Δ post-cracking response for FRC panels via simple approaches. The model proposed in Ref. [20] belongs to this category. It is based on a fixed parabolic softening law ($N = 2$) and was recently used by Ref. [17]. The model neglects the contribution of the elastic part of the sound ligament in tension, and their theory predicts only the behaviour of FRC after ultimate. Theoretical predictions from this model do not correctly predict some of the test results [17,20]. Moreover, it is not conservative and presents energy absorption superior to the test results.

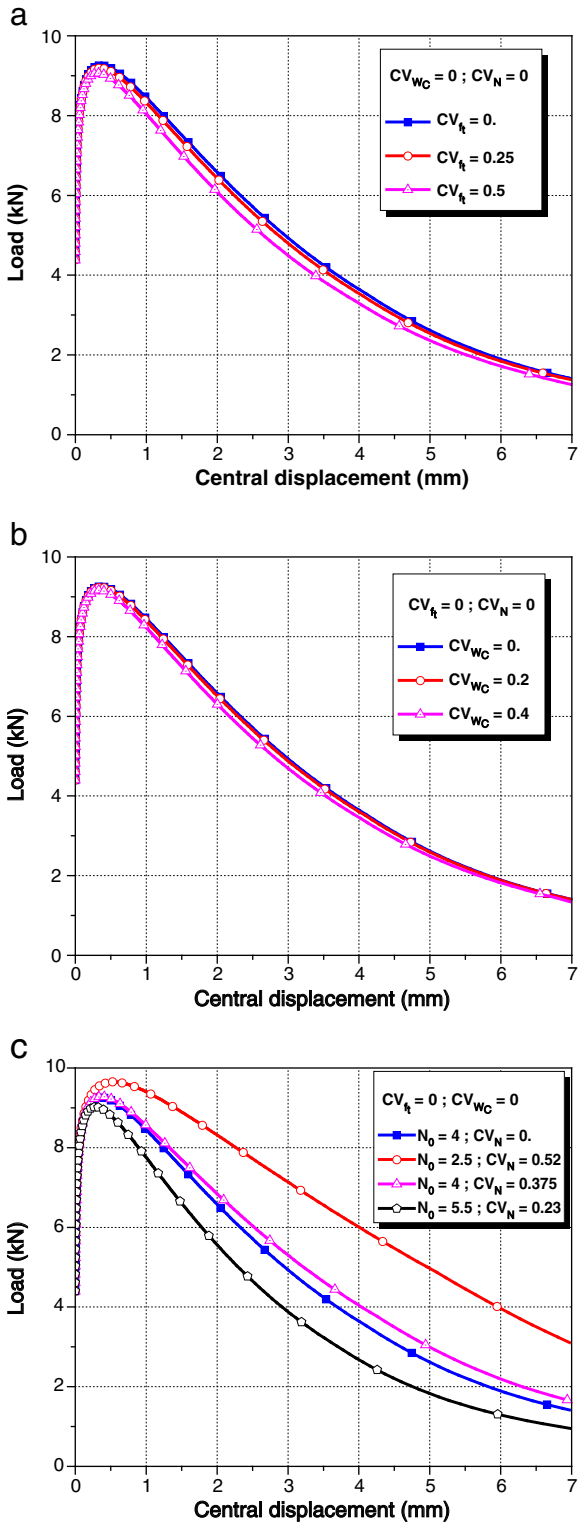

Fig. 6. Mean load displacement curves for beams. a. *ft* variability effect. b. W_C variability effect. c. *N* variability effect.

4.1. Cinematic equations for the round determinate panel test

The ASTM [1] round panel test is one of the tests that exhibits particularly low variability in performance and undergoes a mode of flexural failure that is highly repeatable [30]. When a point load is introduced at the center of a round determinate panel, flexural

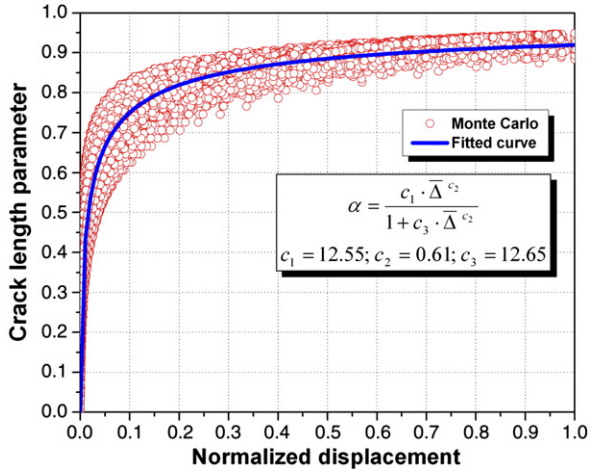

Fig. 7. Crack length parameter-normalized displacement diagram for panels for $h = 75$ mm.

stresses develop in turn leading to the formation of three radial cracks with unequal angles as shown in Fig. 9.

Using yield line theory, Tran et al. [29] developed the following necessary equations that link the crack angle rotation θ to the central

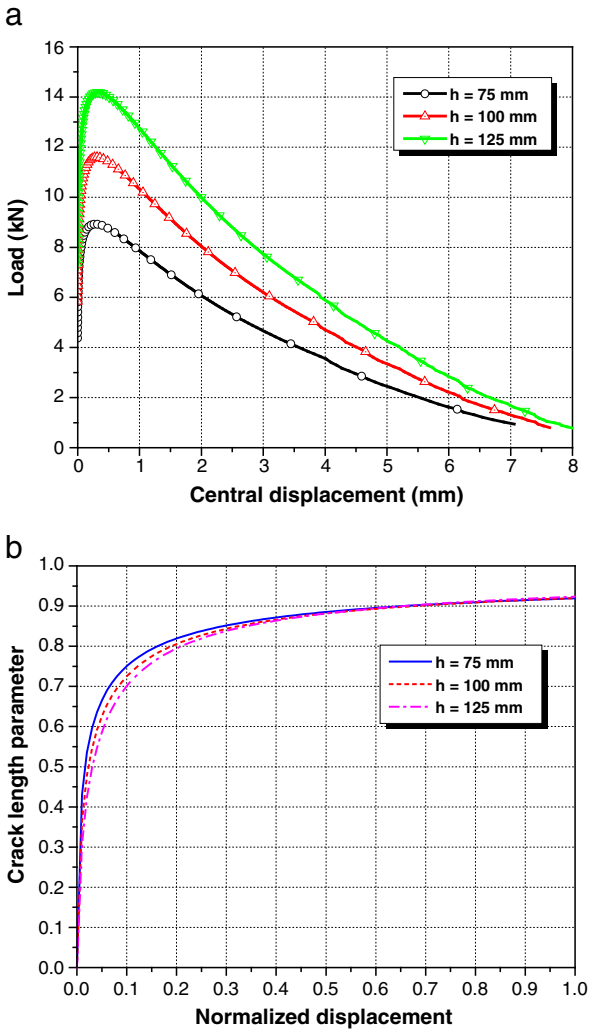

Fig. 8. Generalization to other depths. a. Mean load displacement curves for $N_0 = 4$. b. α–$\overline{\Delta}$ diagrams.

Table 1
Constants of the fitted α–$\bar{\Delta}$ diagram.

	$h=75$ mm	$h=100$ mm	$h=125$ mm
c_1	12.55	12.60	12.70
c_2	0.61	0.67	0.73
c_3	12.65	12.70	12.75

displacement Δ, and the load F to the resisting moment M (Eq. (23)):

$$\theta_i = tan^{-1}(A_i \cdot \Delta) + tan^{-1}(B_i \cdot \Delta); i = 1,3 \quad (23)$$

$$F = \frac{\sum_{i=1}^{3} \theta_i}{\Delta} M \cdot R$$

R is the panel radius, A_i and B_i are constants derived according to Refs. [29] and [30]. They are defined as function of the midpoint angles γ_1, γ_2 and γ_3 of the radius r of C-1550 panel to the supports. For the particular case when $\gamma_1=\gamma_2=\gamma_3=0$, Eq. (23) become (Eq. (24)):

$$\theta = 2\, tan^{-1}\left(\frac{\sqrt{3}}{2r} \cdot \Delta\right) \quad (24)$$

$$F = \frac{3\sqrt{3}}{2}\frac{R}{r}\frac{\theta}{tan(\theta/2)} M$$

4.2. Procedure for deriving F–Δ post-crack response for the round determinate panel

The proposed Eq. (22) constitutes the additional relation that links the crack length parameter α to the deflection Δ. This equation is needed to obtain the complete panels post-cracking load–deflection (F–Δ) response for an arbitrary inputted σ–W diagram. The developed approach for panels is simple and the F–Δ curves are determined according to the following algorithm:

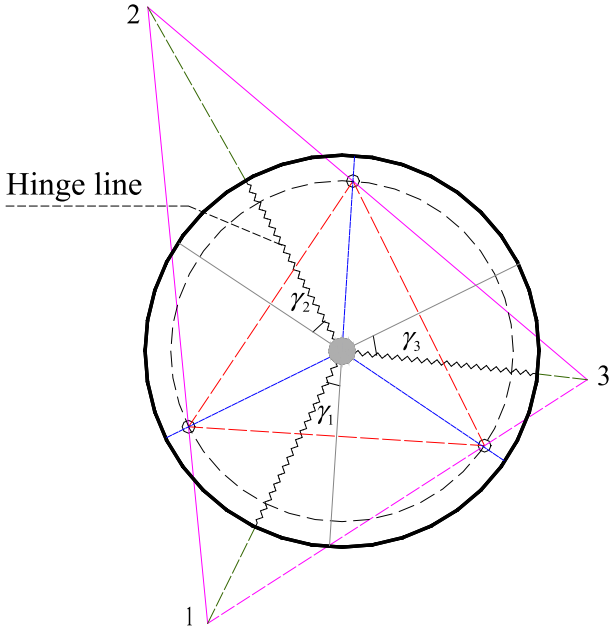

Fig. 9. Failure mechanism at unequal angles for a C-1550 panel (Adapted and revised from Ref. [30]).

(i) The central deflection Δ of the panel is increased. The crack length parameter α is determined according to Eq. (22);
(ii) Using the yield line theory, the crack angle of rotation θ is related to the displacement Δ function of the chosen failure pattern using Eqs. (23);
(iii) The mean crack mouth opening displacement W_{max} is determined according to Eq. (8);
(iv) The tensile zone βh is determined according to Eq. (6);
(v) The resisting moment developed at the yield line is determined according to Eq. (3.b) and is transferred into the load capacity using the yield line theory (Eq. (7)).

It is worthy to note that in Ref. [29] the angle θ is linked to γ_1, γ_2,γ_3 and Δ under the assumption that the height of cracks is equal to the height of specimen, which is not the case in this study as α varies from 0 to 1.

4.3. Comparison with the experimental results

In this section, the theoretical load–deflection curves of the proposed approach are compared to the experimental results. Exhaustive experimental investigation of FRC materials is beyond the scope of this study, and only two types of materials are used for the validation: the FRC60 mix and the FRC35T mix (see Table 2). These panels are selected from 16 panels of an experimental program conducted at Ecole Polytechnique of Montreal on FRC materials including the direct tension and the 3 point-beam bending tests [11].

Fig. 10 illustrates the round determinate panel test setup and the typical failure mechanism for panels D2 and D4 corresponding to the FRC60 mix. The panel radius is 400 mm, the radius to supports is 375 mm, and the thickness is 80 mm. The experimental load–displacement curves for the panels are shown in Fig. 11. As recommended by Bernard [8], they have been corrected to compensate for the amount of friction at the support. The area under the curve represents the actual amount of energy absorbed by the specimen.

Complementary direct tension tests were also performed to derive experimentally the full σ–W diagrams for both FRC mix. Six specimens made from the same FRC mix were tested; the mean curves are shown in Fig. 12.

The σ–W curve is characterised by three main regions. The first region starts at the peak load corresponding to concrete cracking and takes its end at a crack opening around 0.05 mm. For wider cracks, the concrete matrix is inefficient in tension, and the fibres transfer the force via bridging cracks. The second region is characterized by an ascending curve that is more or less important. This region exists only for a high amount of fibres as observed in this research program. The length of this region primarily depends on the fibre type and content, and it is different for the two mixes distribution in the concrete shown in Fig. 12. For the third region, the slope of the curve reduces smoothly accompanied by an asymptotic residual load. As shown by Fig. 11, the test results exhibit a softening behaviour that is different from one test to another. This may be explained by the random fibre mix, and partly by fibres failure. Therefore, the parabolic softening law cannot be used as a general law for characterizing FRC panels as adopted in

Table 2
Mix proportions and properties of the steel FRC.

	FRC35T	FRC60
Cement (kg/m^3)	500	450
Water/cement ratio	0.42	0.44
Sand (kg/m^3)	867	854
Gravel	676	788
Superplasticizer (L/m^3)	10.9	8.5
Fibre volume (kg/m^3)	80	80
Fibre length (mm)	35	60
Fibre dosage (%)	1	1
Fibre length/diameter ratio	65	80

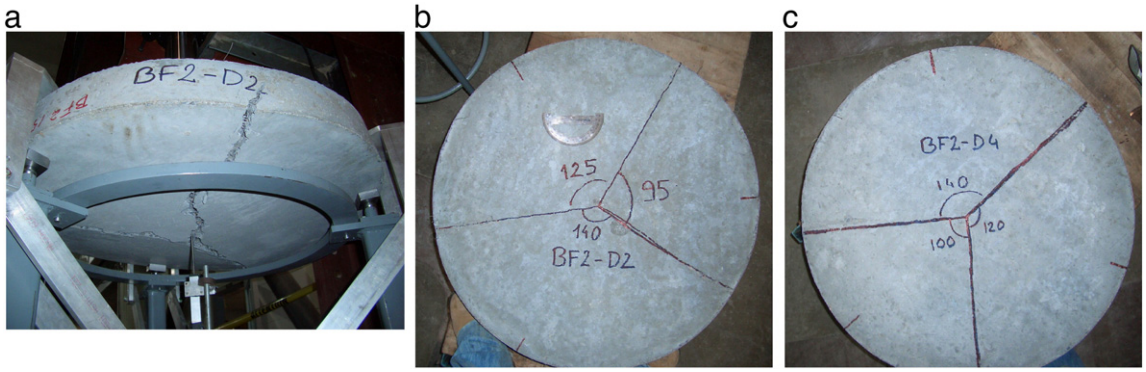

Fig. 10. Test setup and typical failure mechanisms for the FRC60 mix panels.

Marti's model. As reported in Ref. [31], an examination of the experimental load–deflection curves suggests the modeling of the σ–W diagrams by at least a trilinear function: an initial softening part with an abrupt slope, a plastic part, and a final softening part. These three parts would depend on the characteristics of the matrix concrete, bridging of fibre, and pull out of fibre, respectively.

Fig. 13 shows the failure mechanics (hinge lines) for panels D2 and D4. It is noteworthy that the three hinge lines (between each supports) are generally repeatable for almost all the tests, but the midpoint angles γ_1, γ_2 and γ_3 are quite random from one test to another, in which their influence on the load–displacement curve is shown in Fig. 14.

For each tested panel corresponding to a specific FRC mix used in this study, the midpoint angles were measured, and the load displacement curve was calculated using the corresponding σ–W diagram obtained from direct tension tests (Fig. 11). Thereafter, the mean curve is reported in Fig. 14 along with the idealized case of $\gamma_1=\gamma_2=\gamma_3=0$. One sees that, globally, the midpoint angles variation exert little influence on the load displacement curve. For both mixes, one obtains, using the measured angles, a slightly higher capacity and level of softening in comparison to the case with $\gamma_1=\gamma_2=\gamma_3=0$. However, this statement may be different if the plotted mean curve is based on a very big number of panels.

The results obtained from the proposed approach are compared to the experimental results in Figs. 15 and 16. For each FRC mix, the mean softening σ–W diagram obtained from the direct tension test is used as the input for the algorithm described in Section 4.2. It is well illustrated that the mean load displacement curves of the proposed model are inside the area limited by the min–max envelope of the various tests. Furthermore, the model predictions are in good agreement with the whole mean experimental load displacement curve, which confirms the efficiency of the proposed approach.

The proposed approach that is applied for the round determinate panel in this paper can also be easily generalized to a variety of panels following the algorithm described in 4.2 [24]. This study indicates that it is possible to obtain satisfactory predictions of the post-crack load–deflection response for panels with an arbitrary stress–crack width relationship using this present model.

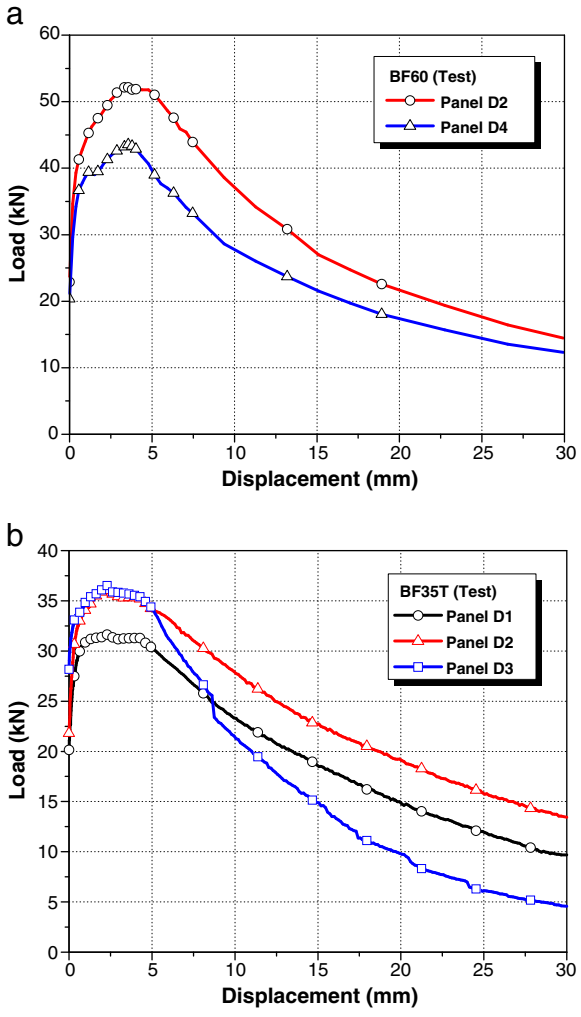

Fig. 11. Experimental load–displacement curves.

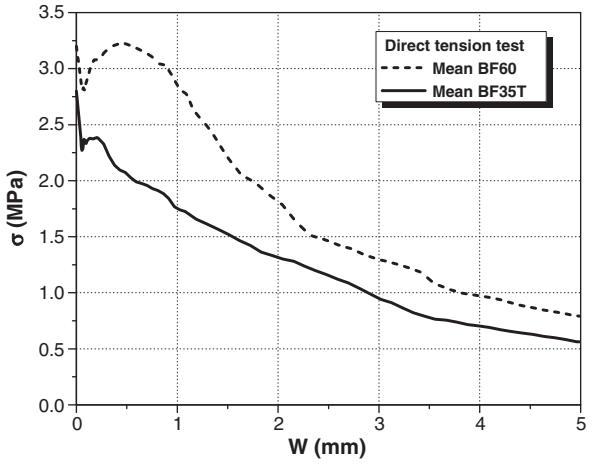

Fig. 12. Mean σ–W diagrams from direct tension test.

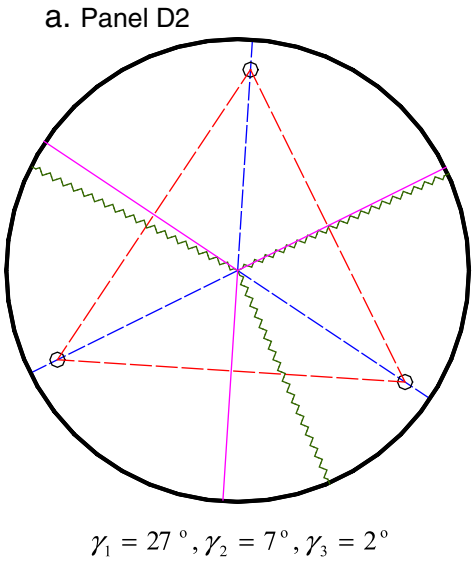

Fig. 13. Failure mechanism of the BF60 FRC mix panels.

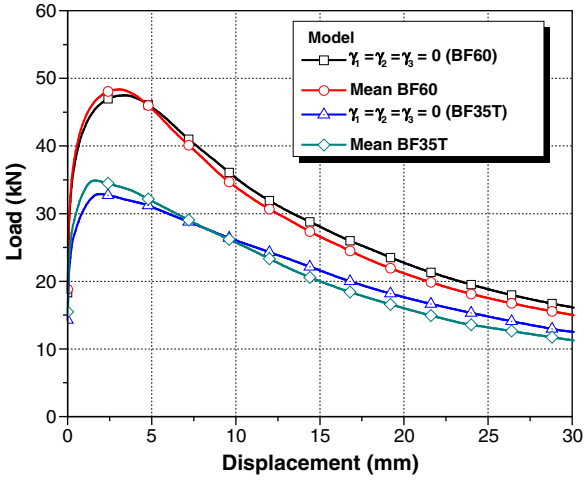

Fig. 14. Midpoint angles influence.

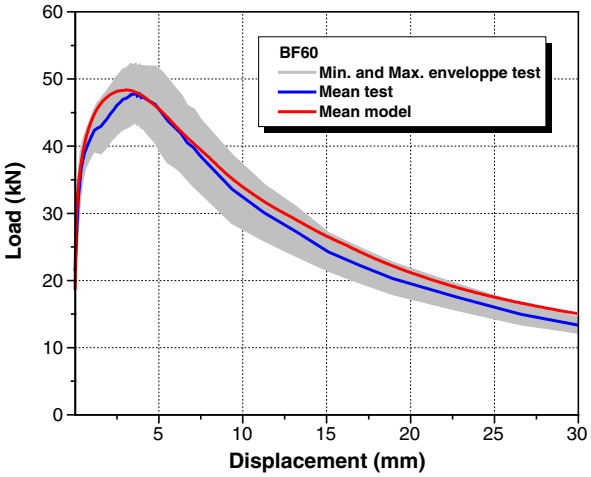

Fig. 15. Model results and comparison with experimental data for FRC60 mix.

5. Conclusion

In this paper, a semi-analytical model aimed at investigating the post-cracking behaviour of FRC panels is proposed. The model is based on the equilibrium of force in the critical cracked section and uses an arbitrary tension softening diagram as the input. In this situation, an additional relation that links the crack length parameter to the deflection is required. Due to the stochastic nature of the material properties, the random fibre distribution, and other uncertainties involved in the concrete mix, deterministic approaches are not suitable for deriving that additional relationship for panels. The resorting to probabilistic techniques enables the modeling of uncertainties and analyzing their dispersion effect. In this context, the load deflection response is predicted using the yield line theory based on the crack length parameter-normalized deflection diagram developed from the analysis of beams having the same thickness using the Monte Carlo simulation (MCS) technique.

The proposed approach was applied to round determinate panels, and results obtained were compared to the experimental results. The mean softening diagrams obtained from the direct tension test were used as the input. It was found that the mean load displacement curves of the proposed model are inside the area limited by min–max envelopes. Furthermore, the model predictions are found in good agreement with the whole mean experimental load displacement curve, which confirms the efficiency of the proposed approach.

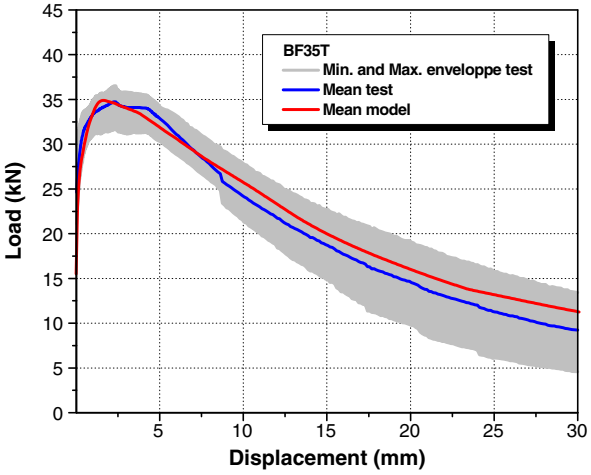

Fig. 16. Model results and comparison with experimental data for FRC35T mix.

Despite the proposed approach that was presented in this paper, which was applied to the round determinate panels, it can also be easily generalized to a variety of panels. This study indicates that it is possible to obtain satisfactory predictions of the mean post-cracking load–deflection response for panels with an arbitrary stress–crack width relationship using the described model.

Acknowledgement

The authors would like to acknowledge the financial support obtained from the Natural Sciences and Engineering Council of Canada.

References

[1] American Society for Testing and Materials (ASTM), Standard test method for flexural toughness of fibre reinforced concrete (using a centrally loaded round panel). American Society for Testing and Materials standard C-1550, West Conshohoken, 2003
[2] American Society for Testing and Materials (ASTM), Standard test method for flexural toughness and first crack strength of fibre reinforced concrete (Using beam with three point loading). American Society for Testing and Materials standard C-1018, West Conshohoken, 1997
[3] J.L. Antunes, R. Gettu, Determining the tensile stress–crack opening curve of concrete by inverse analysis, Journal of Engineering Mechanics ASCE 132 (2) (2006) 141–148.
[4] R. Ballarini, S.P. Shah, L.M. Keer, Crack growth in cement-based composites, Engineering Fracture Mechanics 20 (3) (1984) 433–445.
[5] B. Barragán, R. Gettu, M.A. Martín, R.L. Zerbino, Uniaxial tension test for steel fibre reinforced concrete—a parametric study, Cement & Concrete Composites 25 (2003) 767–777.
[6] Z.P. Bazant, Y.U. Qiang, Z. Goangseup, Choice of standard fracture test for concrete and its statistical evaluation, International journal of fracture 118 (2002) 303–337.
[7] E.S. Bernard, Behaviour of round steel fibre reinforced concrete panels under point loads, Material and Structures Journal, RILEM 33 (2000) 181–188.
[8] E.S. Bernard, The role of friction in post-crack energy absorption of fibre reinforced concrete in the round panel test, Journal of ASTM international, RILEM 2 (1) (2005) Paper ID JAI11771.
[9] J.H. Bungey, S.G. Millard, Testing of concrete structures, Blackie Academic and Professional, Glasgow, UK, 1996.
[10] Q. Chengqing, Quantitative assessment of plastic shrinkage cracking and its impact on the corrosion of steel reinforcement. Ph.D thesis, Perdue University, USA, 2003.
[11] De Montaignac, R., Design of steel fibre concrete elements - from the material to the structure. Ph.D. Thesis, Ecole Polytechnique of Montreal (in press), 2011.
[12] Destrée, X., Structural application of steel fibre as principal reinforcing: conditions – design – examples. Proceeding of the Fifth RILEM Symposium of Fibre-Reinforced Concrete, Lyon, France, September 13–15 2000, pp. 291–301, 2000
[13] European Federation of National Associations of Specialist Contractors and Material Suppliers for the Construction Industry (EFNARC), European specification for sprayed concrete, Aldershot, U.K, 1996.
[14] European Standard, Test method for metallic fibered concrete—measuring the flexural tensile strength, European Committee for Standardization, Brussels, 2005.
[15] K.W. Johansen, Yield line theory, Cement and Concrete Association, U.K., 1972
[16] Dupont, D., and Vandewalle, L., Recommendations for Testing of SFRC: Report of Subtask 7.1: Final Report. Test and Design Methods for Steel for Steel Fibre Reinforced Concrete, Brite Euram BRPR-CT98-0813 Project No: BE 97–4163 (CD-ROM), 2002.
[17] A.R. Khaloo, M. Afsari, Flexural behaviour of small steel fibre reinforced slabs, Cement band concrete composites 27 (2005) 141–149.
[18] N. Kurihara, M. Kunieda, T. Kamada, Y. Uchida, K. Rokugo, Tension softening diagrams and evaluation of properties of steel fibre reinforced concrete, Engineering Fracture Mechanics 65 (2–3) (2000) 235–245.
[19] J.G. MacGregor, S.A. Mirza, B. Ellingwood, Statistical analysis of resistance of reinforced and prestressed concrete members, Journal of the American Concrete Institute 80 (3) (1983) 167–176.
[20] P. Marti, T. Pfyl, V. Sigrist, T. Ulaga, Harmonized test procedures for steel fibre-reinforced concrete, ACI Materials Journal (1999) 676–685 November–December.
[21] S.A. Mirza, M. Hatzinikolas, J.G. MacGregor, Statistical description of strength of concrete, Journal of the structural division ASCE 105 (ST6) (1979) 1021–1037.
[22] S.A. Mirza, J.G. MacGregor, Probabilistic study of strength of reinforced concrete members, Canadian Journal of Civil Engineering 9 (3) (1982) 431–448.
[23] A. Nour, A. Slimani, N. Laouami, Foundation settlement statistics via finite element analysis, Journal Computers and Geotechnics 29 (8) (2002) 641–672.
[24] A. Nour, B. Massicotte, Use of tension softening diagrams for predicting the post-cracking behaviour of steel fibre reinforced concrete panels, Proceedings of the 6th International Conference on Fracture Mechanics of Concrete and Concrete Structures 3 (2007) 1533–1540.
[25] S. Popovics, Strength and related properties of concrete, a quantitative approach, John Wiley and Sons, New York, 1998.
[26] M. Roger, L. Foote, Y.W. Mai, B. Cotterell, Crack growth resistance in strain-softening materials, Journal of the Mechanics and Physics of Solids 34 (6) (1986) 593–607.
[27] RILEM 162-TDF: Test and design methods for steel fibre reinforced concrete – Uniaxial tension test for steel fibre reinforced concrete. Materials and Structures, Vol. 34, pp.3-6, 2001.
[28] Rossi, P., Les betons de fibres metalliques. Final Rep., Bétons de Fibres Métalliques, éléments de structure fonctionnant comme des poutres, AFREM, 1995.
[29] V.N.G. Tran, A.J. Beasley, E.S. Bernard, V.N.G. Tran, A.J. Beasley, E.S. Bernard, Application of yield line theory to round determinate panels, in: E.S. Bernard (Ed.), Shotcrete: Engineering Developments, Swets, and Zeitlinger, Lisse, 2001, pp. 245–254.
[30] V.N.G. Tran, E.S. Bernard, A.J. Beasley, Constitutive modeling of fibre reinforced shortcrete panels, Journal of Engineering Mechanics 131 (5) (2005) 512–521.
[31] Y. Uchida, N. Kurihara, K. Rokugo, W. Koyanagi, Determination of tension softening diagram of various kinds of concrete by means of numerical analysis, in: F.H. Wittmann (Ed.), Fracture mechanics of concrete structures, AEDIFICATIO Publishers, 1995, pp. 17–30.
[32] J. Zhang, H. Stang, Application of stress crack width relationship in predicting the flexural behaviour of fibre-reinforced concrete, Journal Cement and Concrete Research 28 (3) (1998) 439–452.